ELSEVIER

Powder Technology 122 (2002) 136–144

POWDER TECHNOLOGY

www.elsevier.com/locate/powtec

Shear stresses and material slip in high pressure roller mills

K. Schönert *, U. Sander

Institut für Aufbereitung und Deponietechnik, Universität Clausthal, Walther-Nernst-Str. 9, D-38678 Clausthal-Zellerfeld, Germany

Accepted 19 March 2001

Abstract

The compaction of the particle bed in a high pressure roller mill causes pressure and shear forces on the rollers, which have been measured simultaneously with a sensor. As known, the pressure peak arises short above the gap neck, the shear is firstly orientated against and then in the rotation direction. However, the zero point does not coincides with the pressure peak as often said but lies before it. In the entire compression zone and in the first part of the relaxation zone, the shear–pressure ratio is smaller than the coefficient of external friction μ, slip, therefore, does not exist in this region. This ratio exceeds μ only near to the outlet and indicates slip there.

Based on a force balance on a differential strip and with the assumption of proportionality between the transversal pressure in the bed and the normal pressure on the roller, an equation arises relating shear to pressure. Only one property of the granular material remains in this equation, the stress ratio coefficient λ defined as in powder mechanics. The calculated shear agrees well with the measured value in the compression zone until to the shear minimum but is clearly smaller further down. The analysis of the measurements in view of the theoretical considerations leads to the conclusions that slip only exists in the region near to the outlet. Here, the material is extruded, which causes a tensile force acting on the material above and increases by that the shear over the calculation. This effect ceases further up, therefore, the calculation approaches the measured values.

Keywords: Comminution; High pressure roller mill; Shear stresses; Material slip

1. Introduction

Any compaction of a granular material forces the particles to move sidewards. The internal and external friction and, furthermore, the outer confinement determine whether or not they can move and, if they can, in what an extent. However, in all circumstances, shear forces are caused on the surfaces of the compacting tools. Shear forces, therefore, are not a sufficient indication for slip, as often is assumed. Slip happens only if the shear exceeds the external friction; that means the ratio of shear stress τ and pressure p (normal stress) has to exceed the friction coefficient μ.

$$\tau/p = \mu(\text{materials}, \text{surface structure}, \text{moisture}, \text{pressure}, \ldots).$$

The idea of an overall slip in roller mills and briquetting rollers results from the experiences with metal rolling, where the metal bar moves firstly slower than the peripheral roller velocity and then faster. This fact is due to the incompressibility of metals and the law of continuity. However, a particle bed is compressible and that law can be satisfied without slip. However, the compressibility decreases as the compaction increases, therefore, slip may become necessary as the particle bed is compacted highly.

Until now, the only evidence for slip in roller mills follows from the comparison of the theoretical with the experimental throughput. For calculating the theoretical value, the relative bulk density at the gap neck has to be known, which cannot be measured directly and is to be estimated from the flake density. Further problems are the edge effect, the bypassing material squeezed sidewards out off the gap and fluctuations of the gap width, which happens sometimes in industrial operations. The edge effect can cause either a reduced or an enlarged local throughput. The bypass always enlarges the overall throughput. Gap fluctuations lead to an undefined situation. Lim et al. [1] have published a lot of data from diamond, bauxite and gold ores about this comparison taken from experiments with a lab-scale mill and some industrial mills. They have calculated a so-called γ-number defined as:

$$\gamma = \dot{M}/\rho usL = (w_S/u)(\rho_S^*/\rho)$$

* Corresponding author. Tel.: +49-5323-722-241; fax: +49-5323-722-353.

E-mail address: annemarie.holste@tu-clausthal.de (K. Schönert).

0032-5910/02/$ - see front matter
PII: S0032-5910(01)00409-0

where $\dot{M}$ = throughput, ρ = material density, s = gap width, L = roller length, w_S = average material velocity in the gap neck, u = roller speed, ρ_S^* = bulk density in the gap neck. The value of γ can be calculated without any assumption, if the gap width does not fluctuate. It is stated that (w_S/u) would be definitely greater than 1, which indicates slip at the gap neck (extrusion of the material), if γ exceeds 1 because the ratio (ρ_S^*/ρ) has to be smaller than 1. However, this conclusion requires that bypassing material is not included in $\dot{M}$. Most of the lab-scale mill data are below 1 while most of industrial mill data are above 1. The authors suppose an influence of the roller diameter on the extrusion effect. Although this could be possible, theoretical consideration on the problem does not predict a direct influence of the roller diameter as shown later in this paper. It is also likely that the industrial operations do not satisfy the above-mentioned assumption.

For improving the understanding of the slip problem, more theoretical and experimental studies on the stress distribution along the roller surface are needed; these have been the objectives of the work reported here.

Theoretical treatments have been published only for briquetting rollers. The basis papers are those from Katashinskii [2] and Lee and Schwartz [3]. They consider the force balance at a strip element, assumes plane stress and an overall slip except at the neutral line as in metal rolling. The crucial point in these approaches is the formulation of a yield criterion in the material. Katashinskii introduces a yield strength, which has to be met by the difference of the principle stresses; Lee and Schwartz introduces the Coulombian criterion. It is furthermore assumed that the yield stress and the cohesion in the Coulombian criterion, respectively, depend on the compaction. The slip of the strip element causes on both rollers tangential forces, which complete the force balance. They are set to be equal to the coefficient of the external friction multiplied with the normal force acting on the strip. After introducing some additional assumptions, the differential equation is solved with the objective to calculate the pressure distribution on the rollers. It has to be emphasized that these treatments cannot give any evidence on slip because it was already assumed.

The well-known theory of Johanson [4] was developed mainly to predict the operational parameters of briquetting rollers. The material transport within the compaction region is assumed to be slipless; this approach, therefore, also cannot help.

Only a few publications describe measurements of normal and tangential forces, respectively, of pressure and shear, on the rollers. The first paper on measurements of the pressure at metal rolling was published by Siebel and Lueg [5]. The first investigations on pressure and shear at compacting of metal powders have been performed from Chekmarev et al. [6]. Three force transmitters with a pin of 1.2 mm have been used, which flush with the roller surface. These transmitters are inserted with different directions in such a way that the pins detect the force within a narrow surface region. The paper shows measurements in a briquetting roll with 185-mm rollers running very slowly at a speed of 0.024 m/s. The shear is firstly orientated against the rotation, vanishes at the pressure peak and is then orientated with the rotation. The shear–pressure quotient drops down from 0.4 to 0, increases then steeply to a maximum of about 0.5 and falls back again. The problem of slip is not discussed. In the late 1980s, two publications describe measurements of tangential and axial shear at metal rolling: Britten and Jeswiet [7] and Hatamura and Yoneyama [8]. The pressure in roller mills was measured from Feige [9], Andersen [10], and Lubjuhn et al. [11], and in briquetting rolls from Michel et al. [12]. The authors of this paper have published some measurements of pressure and shear in a high pressure roller mill [13] and will discuss here a theoretical consideration as announced, which results are used for analysing the measurements, particularly regarding the slip problem.

2. Experimental work

The experiments were done in a lab-scale mill with smooth rollers of 200 mm diameter and 100 mm length. The fixed roller was equipped with dam rings to avoid bypassing of material. The sensor for measuring simultaneously pressure and shear was milled out of a chrome steel plate and has a two-legged cross-section with an angle of 90°, see Fig. 1. The sensor top is flat and its area A is 10×2 mm^2. Its long side is orientated in axial direction. Strain gauges are glued at both sides of the legs and connected by sliding rings with the electronic unit. The normal and tangential force, F_N and F_T, and by that the

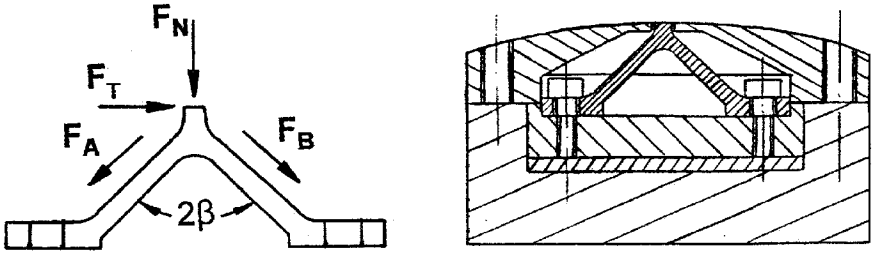

Fig. 1. Sketches of the pressure–shear sensor.

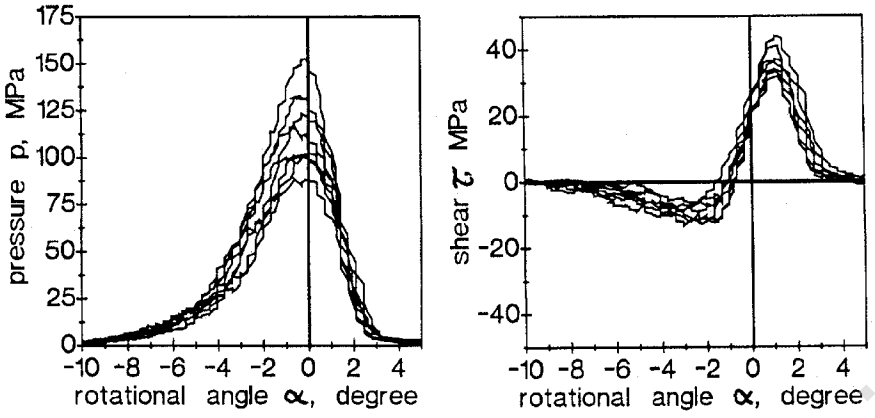

Fig. 2. Pressure and shear of one experiment with 7 revolutions, quartz 1.0/2.0 mm, $F_{sp} = 4.1$ N/mm^2, $u = 1.0$ m/s.

pressure p and the shear τ, follow from the measured force, F_A and F_B, according to:

$$F_N = (F_A + F_B)\cos\beta \qquad F_T = (F_A - F_B)\sin\beta \qquad (1)$$

$$p = F_N/A \qquad \tau = F_T/A \qquad (2)$$

The sensor was designed for $p_{max} = 300$ MPa and $\tau_{max} = 165$ MPa. For measuring the rotation angle, a potentiometric transmitter was connected to the shaft of the fixed roller and adjusted that the angle zero indicates the sensor position in the axis plane. Experiments were done with a quartz fraction 1.0/2.0 mm and a calcite fraction of 0.8/1.2 mm comminuted with a specific milling force $F_{sp} = F/DL$ from 1.5 to 5.4 N/mm^2 at a roller speed u between 0.3 and 2.3 m/s. In each run, 4–10 measurements could be recorded and stored with a transient recorder.

Fig. 2 shows typical curves of one experiment with quartz stressed with a specific milling force of 4.1 N/mm^2 at a roller speed of 1.0 m/s. The step-shaped form of the curves is due to the reading frequency of the transient recorder adjusted to 1 kHz. With this fraction, only about six particles contact the sensor surface of 20 mm^2, therefore, the curves scatter statistically. For further considerations, each set of curves has been averaged (see Fig. 3) to determine the following characteristics: maximum pressure p_{max}, minimum and maximum shear τ_{min} and τ_{max}, the corresponding angles $\alpha_{p,max}$, $\alpha_{\tau,min}$, $\alpha_{\tau,max}$, also the angles at which the compression starts and the relaxation ends α_C and α_R and the angle $\alpha_{\tau,0}$ at which the shear changes its direction. In this example, the values are $p_{max} = 111$ MPa, $\tau_{min} = -10$ MPa, $\tau_{max} = 31$ MPa, $\alpha_{p,max} = -0.3°$, $\alpha_{\tau,min} = -2.6°$, $\alpha_{\tau,max} = +1.1°$, $\alpha_{\tau,0} = -1.0°$, $\alpha_C = -10.5°$, and $\alpha_R = 4.1°$. An essential result is that the shear changes its direction before the maximum pressure is reached and not at $\alpha_{p,max}$ as is said or assumed until now. This was found in all experiments.

For discussing the slip problem, the shear–pressure ratio $|\tau|/p$ has to be considered, which is plotted in Fig. 4 for the same feed fraction stressed with the three specific milling forces of 2.5, 4.1 and 5.4 N/mm^2. This ratio is smaller than 0.3 in the compression zone ($\alpha < 0$) and

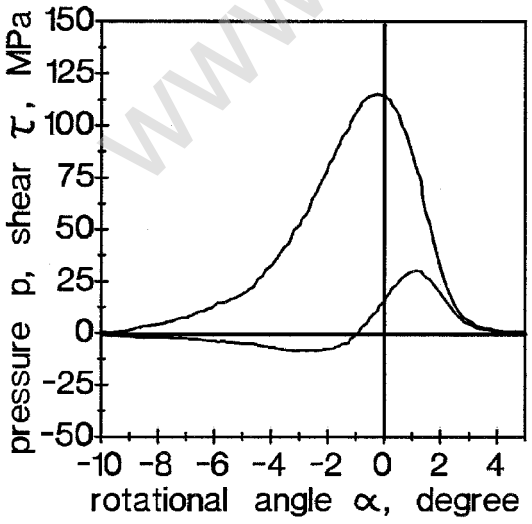

Fig. 3. Average pressure and shear curve of Fig. 2.

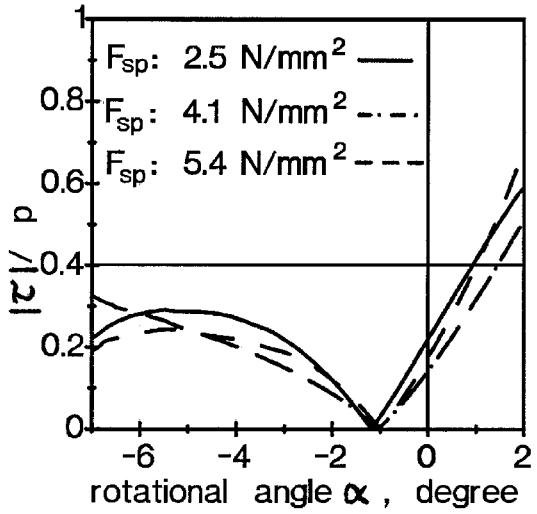

Fig. 4. Shear–pressure ratio, quartz 1.0/2.0 mm, $u = 1.0$ m/s, $F_{sp} = 2.5$, 4.1, 5.4 N/mm^2.

increases up to 0.5–0.7 in the relaxation zone ($\alpha > 0$). If the material would slip, then this ratio should exceed the coefficient of external friction which was measured for this material combination to be about 0.4. Therefore, the material is transported slipless within the compaction zone and the first part of the relaxation zone, and may slip only short before leaving the gap space. This was found in all experiments. In the last part of the relaxation zone, pressure and shear are very reduced, the slip, therefore, will not contribute much to the wear. Regarding a theoretical treatment on the stress distribution, slip should not be included as an assumption as it is done in the theories for briquetting rollers [2,3].

3. Theoretical consideration

In the following, an approach will be developed for describing the stress distribution on the roller surface caused by the compaction of the particle bed. The general problem is that the relevant properties of the particulate material are not well definable, difficult to measure and, above all, change as the bed is compacted and the particles are broken. Therefore, simplifications cannot be avoided. As always, this situation demands experimental proving, which will be done in the next chapter by relating the shear distribution to the pressure distribution without integrating the differential equation. The advantage of this procedure is that only one material property is involved.

The approach starts as usual with the force balance on a strip element s (Fig. 5). This idea includes already the two assumptions that, firstly, the material mass in the element and, secondly, the material properties are not changed by any internal material flow. Fig. 6 shows the position and orientation of the (y,z)-coordinates. Positively signed are all forces and the direction downwards, the shear forces and the angle differential in rotational direction.

The denotations are as follows: angle coordinate α, roller diameter D, roller length L, angular velocity ω, distance between the rollers $a(\alpha)$, gap width $s = a(\alpha = 0)$, roller speed u, material speed w, material density ρ, material bed density (bulk density) ρ^*, relative bulk density δ, relative slip S, gravity acceleration g, accelerating number ζ, pressure (normal stress) on the roller p, shear on the strip element τ, vertical pressure in the material p_z, strip volume $\mathrm{d}V$, strip wall area $\mathrm{d}A_W$ and strip cross-section A_S.

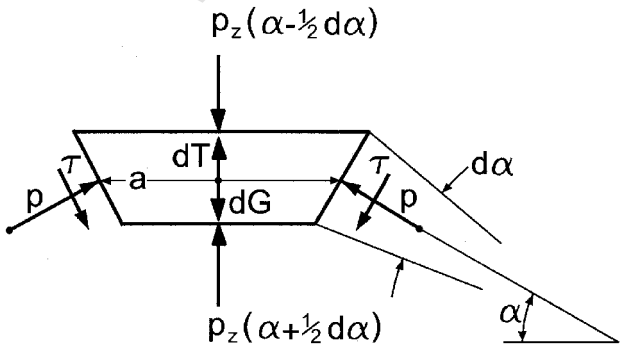

Fig. 5. Force balance on a strip element.

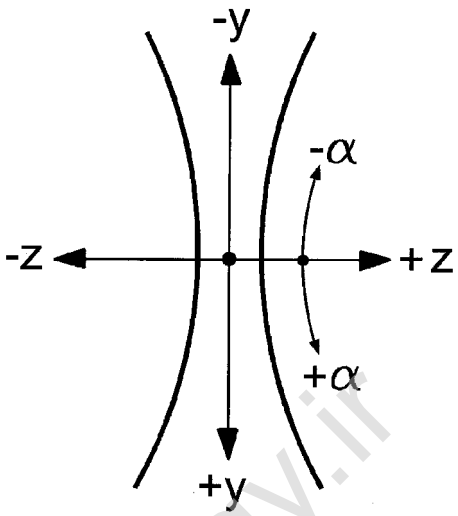

Fig. 6. Coordinates.

The force balance includes the following forces and reads, *s.* (Fig. 5):

gravity force	$\mathrm{d}G = +\rho^* g \mathrm{d}V$
inertia	$\mathrm{d}T = -\rho^* \dot{w} \mathrm{d}V$
shear force	$\mathrm{d}F_\tau = +\tau \cos\alpha \mathrm{d}A_W$
pressure force	$\mathrm{d}F_p = +p \sin\alpha \mathrm{d}A_W$
transverse force	$\mathrm{d}F_z = -(\mathrm{grad}\ p_z A_S)\mathrm{d}z$

$$\mathrm{d}G + \mathrm{d}T + \mathrm{d}F_\tau + \mathrm{d}F_p + \mathrm{d}F_z = 0 \quad (1)$$

It should be noted here that the shear force could also include the friction if the material would slip.

Compression and relaxation zone are small ($|\alpha| < 0.2$), therefore, the following approximations can be used: $\sin\alpha = \alpha$; $\cos\alpha = 1$; $(1 - \cos\alpha) = (1/2)\alpha^2$. Now, Eq. (1) can be written as:

$$\rho^*(g - \dot{w})\mathrm{d}V + (\tau + p\alpha)\mathrm{d}A_W - (\mathrm{grad}\ p_z A_S)\mathrm{d}z = 0 \quad (2)$$

The differential terms $\mathrm{d}V$, $\mathrm{d}A_W$ and $\mathrm{d}z$, and A_S can be given in terms of α and $\mathrm{d}\alpha$, so Eq. (2) can be rewritten as a differential equation in α. The relations are as follows:

$$A_S = aL \qquad a = s + D(1 - \cos\alpha) \qquad s_{rel} = s/D$$
$$a = D\{s_{rel} + (\alpha^2/2)\} = k(\alpha)D$$

$$A_S = k(\alpha)DL \quad (3)$$

$$\mathrm{d}V = A_S(D/2)\mathrm{d}\alpha = (k(\alpha)/2)D^2 L\,\mathrm{d}\alpha \quad (4)$$

$$\mathrm{d}A_W = 2L(D/2)\mathrm{d}\alpha = DL\,\mathrm{d}\alpha \quad (5)$$

$$\mathrm{d}z = (D/2)\cos\alpha\,\mathrm{d}\alpha = (D/2)\mathrm{d}\alpha \quad (6)$$

$$\mathrm{grad}(p_z A_S)\,\mathrm{d}z = A_S\,\mathrm{d}p_z + p_z\,\mathrm{d}A_S + DL\{k(\alpha)\,\mathrm{d}p_z + p_z\,\mathrm{d}k(\alpha)\}$$

$$k = s_{rel} + (\alpha^2/2) \qquad \mathrm{d}k = \alpha\,\mathrm{d}\alpha$$

$$\mathrm{grad}(p_z A_S)\,\mathrm{d}z = DL\{k(\alpha)\,\mathrm{d}p_z + p_z\alpha\,\mathrm{d}\alpha\} \tag{7}$$

Lastly, the acceleration $\dot{w}$ of the strip element has to be arranged in a form fitting consistently in the differential equation. This is possible with the definition of the relative slip S.

$$S = (w - u\cos\alpha)/u\cos\alpha \tag{8}$$

$$w = u(1+S)\cos\alpha$$

$$\dot{w} = (\mathrm{d}w/\mathrm{d}\alpha)(\mathrm{d}\alpha/\mathrm{d}t) = \omega(\mathrm{d}w/\mathrm{d}\alpha)$$

$$\dot{w} = u\omega\{-(1+S)\sin\alpha + S'\cos\alpha\} = u\omega\{-(1+S)\alpha + S'\} \tag{9}$$

With $u = (D/2)\omega$ and $\zeta = (D/2g)\omega^2$ follows:

$$\dot{w} = \zeta g\{-(1+S)\alpha + S'\} \tag{10}$$

The term $(-\zeta\ g\ \alpha)$ represents the acceleration without slip because the strip velocity increases as the z-component of the roller speed.

The bulk density ρ^* can be replaced considering the law of continuity.

$$\rho^*(\alpha)\,a(\alpha) = \rho\delta(\alpha)\,k(\alpha)\,D = \rho\delta(\alpha_C)\,k(\alpha_C)\,D = \rho\delta_C\,k_C\,D \tag{11}$$

With that, the term $\rho^*\mathrm{d}V$ reads as:

$$\rho^*\,\mathrm{d}V = (1/2)\,\rho\delta_C\,k_C\,D^2 L\,\mathrm{d}\alpha \tag{12}$$

Including Eqs. (3)–(12) in Eq. (2) yields:

$$\mathrm{d}p_z - (1/k)\{(p - p_z)\alpha + \tau + (1/2)\,\rho g D\delta_C\,k_C(1 - \zeta(-(1+S)\alpha + S'))\}\mathrm{d}\alpha = 0 \tag{13}$$

The term $(\rho\ \delta_C\ g\ D)$ represents the pressure p_0 of a particle column of height D and the bulk density $(\rho\ \delta_C)$, without wall friction. Now, Eq. (13) reads as:

$$\mathrm{d}p_z - (1/k)\{(p - p_z)\alpha + \tau + p_0(k_C/2)(1 - \zeta(-(1+S)\alpha + S'))\}\mathrm{d}\alpha = 0 \tag{14}$$

This is a differential equation for p_z and comprises the three functions $p(\alpha)$, $\tau(\alpha)$ and $S(\alpha)$, which are not known per se. For this reason, Eq. (14) cannot be solved without introducing additional assumptions. Firstly, it appears reasonable to neglect the weight and inertia expressed in the last term. Taking usual values of $\rho = 3000\ \mathrm{kg/m^3}$, D = 1.5 m, $s_{rel} = 0.02$ and $\alpha_C = 0.2$, the term $(p_0\ k_C/2)$ is only 450 Pa $= 4.5 \times 10^{-4}$ MPa. The number of the bracket can be estimated being below 1000, for example is results 399 with $\zeta = 2$, $\alpha = 0$ and $S' = 2/0.01 = 200$. The last term remains definitely smaller than 1 MPa, but p and τ exceed strongly this value within the essential part of the compression and relaxation zone. Only near at the entry and exit the inertia may have some influence. Neglecting the last term it follows:

$$\mathrm{d}p_z - (1/k)\{(p - p_z)\alpha + \tau\}\mathrm{d}\alpha = 0 \tag{15}$$

Mill size, material bulk density and the compression angle are vanished. The only parameter in the equation is the relative gap width s_{rel}, which, however, depends on material properties, the surface structure, the specific milling force and the roller speed. Also, the slip function $S(\alpha)$ is eliminated; however, the functions $p(\alpha)$ and $\tau(\alpha)$ remains. Although the pressure distribution could be estimated with the compressibility of the material by transferring piston press experiments to the compaction in the gap space, nevertheless, the equation cannot be solved because the shear distribution $\tau(\alpha)$ is unknown. The assumption $\tau = \mu p$, as it is introduced in the theories of Refs. [2,3], requires an overall slip, which would be an arbitrary surmise and not satisfied by the reported measurements. The lack of knowledge about the shear distribution obstructs to treat the problem by solving a differential equation. However, Eq. (15) can be used for relating $p(\alpha)$ and $\tau(\alpha)$ to each other, if $p_z(\alpha)$ can be expressed as a function of $p(\alpha)$. This idea sounds reasonable because the compaction is caused by the pressure p and the compaction creates the transversal pressure p_z. Then, the shear is needed to complete the force balance. Regarding the slip, it is to state that slip requires $\tau > \mu p$. The further approach, therefore, is to find a relation for $p_z(p)$, to introduce this in Eq. (15), to rearrange the equation as a relation $\tau = \tau(p)$, to calculate τ as a function of α by using an estimated or measured pressure distribution and, finally, to determine the region with $\tau > \mu p$ or to compare the calculated and measured shear distribution.

A possibility for relating p_z to p can be adopted from powder mechanics. In the theory on designing hoppers for granular material, the horizontal pressure is related to the vertical pressure by a term called horizontal load ratio λ, which value lies between the Poisson number of the material and 1; $\lambda = 1$ indicates a behaviour like a fluid. The hopper walls confine the horizontal displacement of the material. This idea should be transferred to the problem here and λ denoted as the stress ratio coefficient. However, there are two uncertainties; firstly, the confinement of the material displacement in z-direction and, secondly, the reversibility of λ. Regarding the confinement, it could be argued that this is acceptable as long as the material does not slip because the internal friction exceeds always the external friction. The reversibility of λ means that it depends only on p but is not affected whether p increases or decreases, which possibly can be; however, no data are available. Now, p_z should be replaced by p according to:

$$p_z = \lambda p\cos\alpha = \lambda p \tag{16}$$

The λ-value depends on the material, the particle size distribution and the package structure. The last two characteristics change with the rotational angle α.

$$p_z(\alpha) = \lambda(\alpha)\, p(\alpha) \quad \mathrm{d}\, p_z = p\mathrm{d}\lambda + \lambda \mathrm{d}\, p \tag{17}$$

Eq. (15) now is rewritten as:

$$p\mathrm{d}\lambda + \lambda \mathrm{d}\, p - (1/k)\{\, p(1-\lambda)\,\alpha + \tau\}\mathrm{d}\,\alpha = 0 \tag{18}$$

In the following, the pressure p_R and the shear τ_R on the roller surfaces will be considered which are $p_R = p$ and shear $\tau_R = -\tau$.

$$\tau_R = -k\{\lambda(\mathrm{d}\, p/\mathrm{d}\,\alpha) - p(\mathrm{d}\lambda/\mathrm{d}\,\alpha)\} + (1-\lambda)\, p\alpha \tag{19}$$

As already mentioned, this treatment leads to an equation with only one material property, which is the stress ratio coefficient λ and its dependence on the compaction. Furthermore, only one operational parameter, the relative gap width s_{rel}, is included in the equation. The mill size does not influence directly the (τ, p)-relation, which must be the same for different mills as long as s_{rel} and $\lambda(\alpha)$ are equal. The gap width s can easily be measured; therefore, s_{rel} is known.

An interesting point of this equation is that the shear does not vanish necessarily at the pressure maximum given with $(\mathrm{d}\, p/\mathrm{d}\,\alpha) = 0$. The arguments are that around $\alpha_{p,\max}$, the compaction is almost constant; therefore, the λ-coefficient is also constant, which leads to $(\mathrm{d}\lambda/\mathrm{d}\,\alpha) = 0$, and it follows:

$$\tau_R(\alpha_{p,\max}) = (1-\lambda)\, p\alpha_{p,\max} \tag{20}$$

The pressure reaches its maximum short above the gap neck at a negative α-value; for example, in Fig. 2, the value of $\alpha_{p,\max}$ is $-0.3°$.

$$\tau_R(\alpha_{p,\max}) = -(1-\lambda)\, p|\alpha_{p,\max}| \tag{21}$$

All measurements, however, show a positive shear at $\alpha_{p,\max}$ instead of negative ones according to that equation.

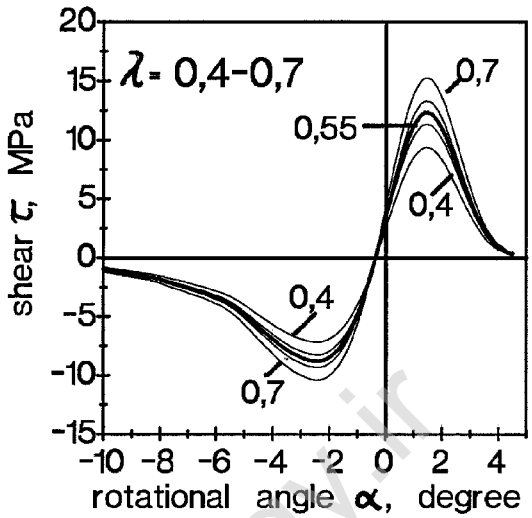

Fig. 8. Influence of λ on the calculated shear, data as in Fig. 2.

Therefore, additional effects, which are not included in these considerations, must exist. This problem will be discussed later.

4. Comparison with experimental results

For calculating the shear with Eq. (19) from a measured pressure distribution $p(\alpha)$, the stress ratio coefficient λ and its dependence on the compaction have to be known. λ-values for particle beds without compaction have been measured for a large number of materials [14]; the values are in the range of 0.34–0.65. However, no data are available for highly compacted beds. In principle, λ reduces and should converge against the Poisson number as the porosity approaches zero. For a first test, therefore, λ is assumed being constant and chosen according to a good fit to the measured shear curve.

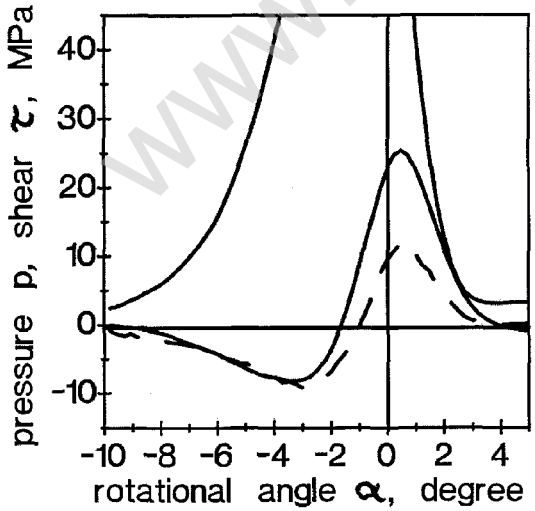

Fig. 7. Comparison of measured (—) and calculated (---) shear, date as in Fig. 2, $\lambda = 0.60$.

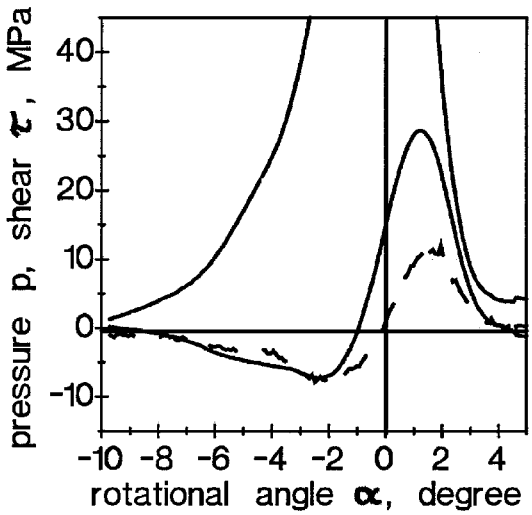

Fig. 9. Comparison of measured (—) and calculated (---) shear, quartz 1.0/2.0 mm, $F_{sp} = 4.1$ N/mm^2, $u = 0.3$ m/s, $\lambda = 0.49$.

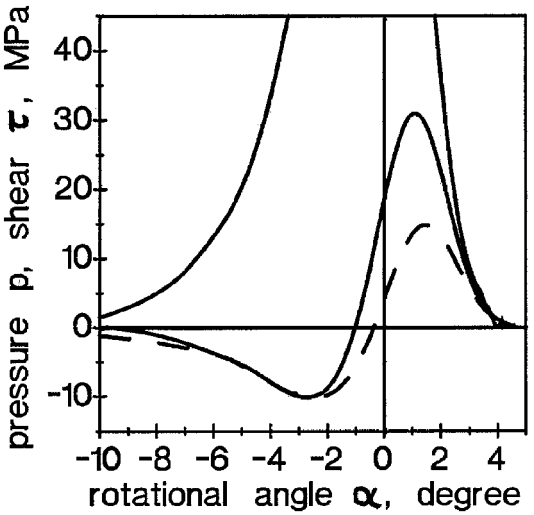

Fig. 10. Comparison of measured (—) and calculated (---), shear, quartz 1.0/2.0 mm, $F_{sp} = 4.1$ N/mm^2, $u = 2.1$ m/s, $\lambda = 0.55$.

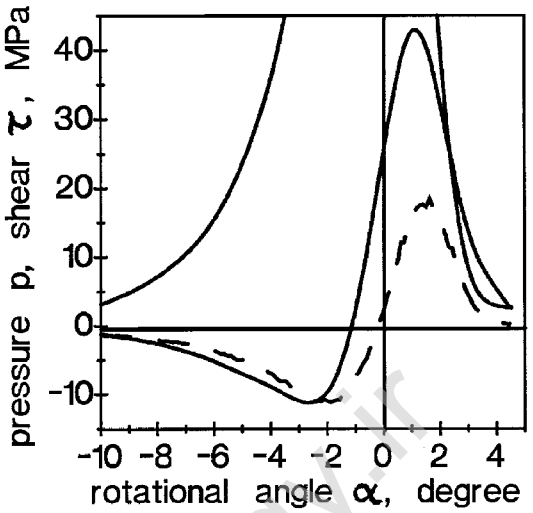

Fig. 12. Comparison of measured (—) and calculated (---), shear, calcite 0.8/1.2 mm, $F_{sp} = 4.3$ N/mm^2, $u = 1.0$ m/s, $\lambda = 0.40$.

Fig. 7 shows the measured and calculated shear for the experiment plotted in Fig. 3. The value of λ was taken as 0.55. The calculated and measured curves fit well until the shear minimum but deviate strongly afterwards.

Particularly, the angle at which the shear vanishes does not agree with the measurement and is located nearer to the gap neck at the angle of $-0.2°$, shortly below $\alpha_{p,max}$ of $-0.3°$, but the measurements gives $\alpha_{\tau,0} = -1.0°$. In order to see the influence of λ, τ-curves for the same experiment have been calculated for $\lambda = 0.4–0.7$, see Fig. 8. As expected, λ influences mainly the extreme values but not the position of $\tau = 0$. However, even with the unreasonable λ-value of 0.7, a great difference remains between the measured and calculated maximum shear.

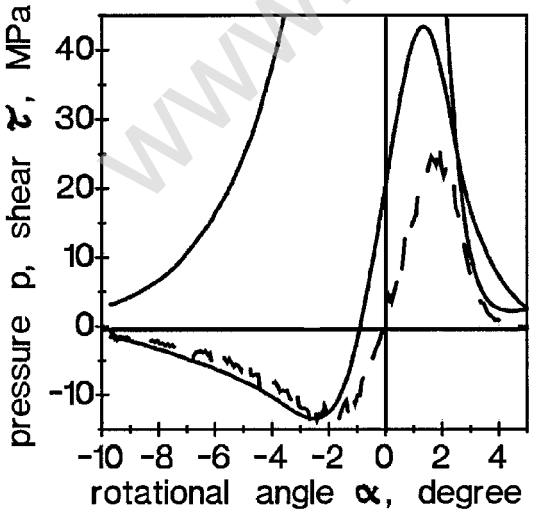

Fig. 11. Comparison of measured (—) and calculated (---), shear, calcite 0.8/1.2 mm, $F_{sp} = 4.4$ N/mm^2, $u = 0.3$ m/s, $\lambda = 0.48$.

The curves in Fig. 8 show that an angle depending λ-value will not improve essentially the agreement with the measurements in the range from α_C to $\alpha_{\tau,min}$. It seems, therefore, sufficient to assume a constant λ-value, which fits τ_{min} to the measurements.

The comparison for all experiments with the quartz and calcite fraction at different speeds and specific milling forces, respectively, shows always the same picture; some examples are given in Figs. 9–12. The λ-numbers for quartz range in 0.49–0.65 with an average of $\lambda = 0.57$ and for calcite in 0.40–0.66 with $\lambda = 0.57$. The measurements with uncompacted particle beds reported in Ref. [14] give $\lambda = 0.52$ for quartz and $\lambda = 0.42$ for calcite. The values for quartz taken from the roller mill experiments agree nicely with direct measurements; those for calcite are somewhat higher.

5. Discussions and conclusions

The comparison of the shear curves shows one region, in which the calculated and measured shear agree well, and another one with a remarkable discrepancy. The right side of Eq. (19) does not include friction. Therefore, the assumption of a slipless transport is not wrong in the first region between α_C and $\alpha_{\tau,min}$. However, what could be the reason for the discrepancy further down?

Firstly, there are some remarks regarding measurement failures. The accuracy of the sensor is very good and better than $\pm 3\%$. However, it could be argued that dust is pressed into the very narrow gap of 100 μm between the sensor tongue and the housing, and blocks the tangential displacement of the tongue, which would cause lower readings instead of higher ones as measured. Measurement failures, therefore, can be excluded. Regarding the block-

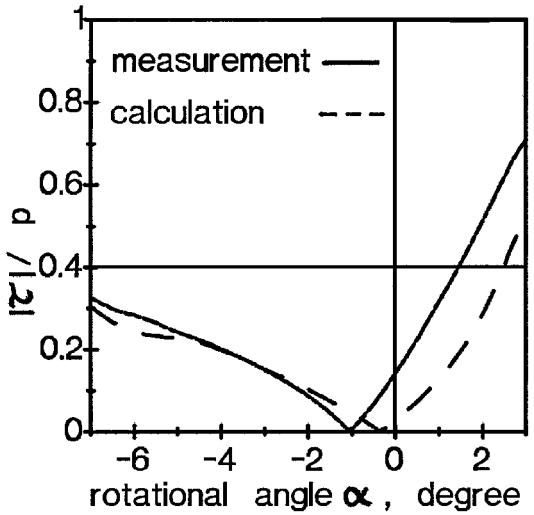

Fig. 13. Measured (---) and calculated (. . .) shear–pressure ratio, data as in Fig. 2, $\lambda = 0.60$.

ing effect, it should be added that this happens time by time and could always detected because strange curves arise. Then, the sensor gap was cleaned.

The higher measured shear in the second region could be caused by a material slip in rotational direction, which would be indicated by a (τ/p)-ratio greater than the coefficient of the external friction. This can be found in the lower part of the relaxation zone but not around the gap neck. It seems, therefore, reasonable to subdivide the region of discrepancy in one part with slip and another one without it. Slip is enforced by tangential forces resulting from the force balance, which leads to Eq. (19). The ratio of calculated shear to pressure, therefore, must exceed the coefficient of external friction. In Fig. 13, $|\tau|/p$ and $|\tau_{cal}|/p$ are plotted with the data of Fig. 2. The second one becomes zero later than the first one but increases then more steeply and reaches also values above 0.4 as the $|\tau|/p$-ratio. Slip, therefore, will exist in the lower part of the relaxation zone; the material transport becomes comparable with an extrusion causing a tensile force in y-direction, which is not included in the force balance and not by that in Eq. (19). This tensile force creates an additional tangential force on the rollers as long as the strength of the compacted bed, which has become a fairly strong flake, can carry it. Then, the sensor measures a higher shear than calculated with Eq. (19).

It should be emphasized that this idea is offered as a hypothesis. More experimental and also theoretical researches are needed to improve the understanding of this phenomenon. However, this could not be done in the frame of this work.

The analysis of the measurements in the view of the theoretical considerations leads to the conclusion that a material slip only exists near to the outlet in the relaxation zone and that no slip is possible around the gap neck ($\alpha = 0$).

The experiences from metal rolling cannot simply be transferred to roller mills and probably also not to briquetting rollers. Any theoretical approach assuming slip does not describe the stress and shear in a high pressure roller mill. The slip in the last part of the relaxation zone causes a tensile force on the material above and increases by that of the shear on the rollers. If this force is not included in the force balance, then the stress distribution on the roller surface cannot be predicted correctly in the entire gap space.

The supposed tensile force could also explain that the pressure reaches its maximum short above the gap neck although the material does not slip at $\alpha = 0$. The tensile strains the flake in z-direction and reduces its thickness and the reaction force of the bed, which causes the pressure on the rollers.

Acknowledgements

This research was supported financially by the Deutsche Forschungsgemeinschaft (DFG). The authors are very grateful for this help.

References

[1] W.I.L. Lim, J.J. Campbell, L.A. Tondo, Extrusion effects in the high pressure grinding rolls, in: S.K. Kawatra (Ed.), Comminution Practices, SME, Littleton, USA, 1997, pp. 293–301.
[2] V.P. Katashinskii, Analytical determination of specific pressure during the rolling of metal powders, Poroshkovaya Metallurgiya (1966) 1–10.
[3] R.S. Lee, E.G. Schwartz, An analysis of roll pressure distribution in powder rolling, International Journal of Powder Metallurgy (1967) 83–92.
[4] J.R. Johanson, A rolling theory for granular solids, Journal of Applied Mechanics, (1965) ASME paper, 65-APMW-16.
[5] E. Siebel, W. Lueg, Untersuchungen über die Spannungsverteilung im Walzenspalt, Mitteilung der KWI 15 (1933) 1–14.
[6] A.P. Chekmarev, P.A. Klimenko, G.A. Vinogradov, Investigations of specific pressure, specific friction and the coefficient of friction during metal powder rolling, Poroshkovaya Metallurgiya (1963) 26–30.
[7] D.D. Britten, J. Jeswiet, A sensor for measuring normal forces with through and transverse friction forces in the roll gap, North American Manufacturing Research Conference Proceedings (1986) 355–359.
[8] Y. Hatamura, T. Voneyama, Measurements of actual stress and temperature on a roll surface during rolling, JSME International Journal (1988) 465–469.
[9] F. Feige, Zur Messung des Druckverlaufs bei der Beanspruchung einer Körnerschicht zwischen zwei Walzen, Aufbereitungs-Technik 30 (1989) 593–599.
[10] K.T. Andersen, Experimental measurements of pressure distribution in cement roller presses, 9th Int. Conf. on Experimental Mechanics, University of Denmark, 1990.

[11] U. Lubjuhn, U. Sander, K. Schönert, Druckprofil in der Kompressionszone der Gutbett-Walzenmühle, Zement-Kalk-Gips 47 (1994) 192–199.
[12] B. Michel, J.P.K. Seville, P. Guigon, C. Sidawy, Experimental study of the roll compaction of powders, Proceedings Sixth Intern. Symp. Agglomeration. 1993, pp. 790–795.
[13] U. Sander, K. Schönert, Pressure and shear on the roller surfaces of high pressure roller mills, Proceedings, International Mineral Processing Congress, 9th A (2000) A4–A97.
[14] A. Kwade, D. Schulze, J. Schwedes, Determination of the stress ratio in uniaxial compression tests, Powder Handling & Processing 6 (1994) 61–65 and 199–203.